Supporting Information

Nakamura *et al.* 10.1073/pnas.0709822105

SI Text

Methods. ***Preparation of the oxidized forms.*** Protein solutions for crystallization were adjusted to 10 mg/ml in 20 mM Tris·HCl, pH 7.5. The crystallization was performed by the hanging-drop vapor-diffusion method with the reservoir solution containing 100 mM sodium acetate, pH 4.8, 200 mM $CaCl_2$, 10% (vol/vol) isopropyl alcohol, and 1 mM DTT (condition 1). The hypervalent sulfur and sulfinic acid forms were prepared by soaking the crystals in a solution containing 100 mM sodium acetate, pH 4.8, 200 mM $CaCl_2$, 10% (vol/vol) isopropyl alcohol, 25% (vol/vol) glycerol, and 1 mM H_2O_2 for 1 min and 1 week, respectively. Soaking in the buffer containing 0.1 mM H_2O_2 instead of 1 mM H_2O_2 for 1 min generated crystals of the preoxidation form. The sulfonic acid form was obtained by incubating ApTPx solution (10 mg/ml protein in 20 mM Tris·HCl, pH 7.5, 1 mM H_2O_2) at 80°C for 20 min before the crystallization. To improve the resolution, we performed the crystallization with a second reservoir solution containing 100 mM imidazole-HCl, pH 6.5, 1 M sodium acetate salt, and 1 mM DTT (condition 2). The hypervalent sulfur form was obtained by soaking the crystal for 1 min in the solution containing 100 mM imidazole-HCl, pH 6.5, 1 M sodium acetate salt, 1 mM H_2O_2, and 25% (vol/vol) ethylene glycol. The data obtained from the crystal grown in condition 2 are presented in the main text as the hypervalent sulfur intermediate because of obtaining higher-resolution data from that condition.

Results and Discussion. ***Oxidation of the peroxidatic cysteine residue.*** As described in the main text, we observed different structures of ApTPx associated with the H_2O_2-mediated oxidation. Fig. S1 shows the side chains of C_p50 in the multiple oxidation states of ApTPx. We observed one, two, and three oxygen atom(s) in the hypervalent sulfur, sulfinic acid, and sulfonic acid forms, respectively (Fig. S1 *e, f,* and *g*). The side chain of the preoxidation form, as well as the reduced form, was not attached to the extra oxygen atom (Fig. S1 *c* and *d*).

Structural comparison of the hypervalent sulfur forms in different crystallization conditions. We obtained the structural data for the hypervalent sulfur form from two crystallization conditions, as described in *SI Text, Methods*. Here, we assign form 1 as the structure determined at a 2.0 Å resolution from the crystal grown at pH 4.8 (condition 1), and form 2 as the structure determined at 1.77 Å in pH 6.5 (condition 2), which is presented as the hypervalent sulfur form in the main text.

The two forms had essentially the same structures with rmsd values of 0.27 Å for 2,360 Cα atoms. As for the detailed structure of the sulfurane portion, the bond lengths coincided well with each other, both of which were interpreted as a mixture of sulfurane derivatives bearing neutral and protonated imidazole moieties (Fig. S2). The two forms showed differences in their bond angles: the values of form 1 were closer to the calculated values of the sulfurane derivative than to those of form 2. Form 1 was obtained by oxidation in the same buffer condition as the preoxidation and sulfinic acid forms. Soaking in the lower concentration of hydrogen peroxide produced the preoxidation form, whereas prolonged oxidation generated the sulfinic acid form (*SI Text, Methods*). These indicate that the hypervalent sulfur form is not an artifact, but an on-pathway intermediate of the oxidation of ApTPx.

Conformational variations with the reaction step. We can correlate the conformational variation with the reactivity of ApTPx in each form. A flexible loop around Glu-119 exhibits different properties associated with the H_2O_2-mediated oxidation of ApTPx (Fig. S3). In the reduced and sulfonic acid forms, Glu-119 interacts with Glu-146 and the flexible loop is in the closed conformation (Figs. S3 *a* and *e*). On the other hand, the flexible loop is disordered in the preoxidation, hypervalent sulfur, and sulfinic acid forms (dashed lines in Fig. S3 *b–d*). The configuration of the side chain of Arg-126 is also different depending on the reaction steps. The basic side chain of Arg-126 is oriented inside the molecule and is in contact with Glu-53 in the reduced and sulfonic acid forms (Fig. S3 *a* and *e*). In the preoxidation, hypervalent sulfur, and sulfinic acid forms, Arg-126 comes to the molecular surface by interacting with C_p50 residue (Fig. S3 *b–d*). The conformational variations described above are correlated with the accessibility of the electrophilic substrate, H_2O_2, to the active site; H_2O_2 tends to contact the active site in the intermediate forms rather than in the fully reduced or sulfonic acid oxidation states.

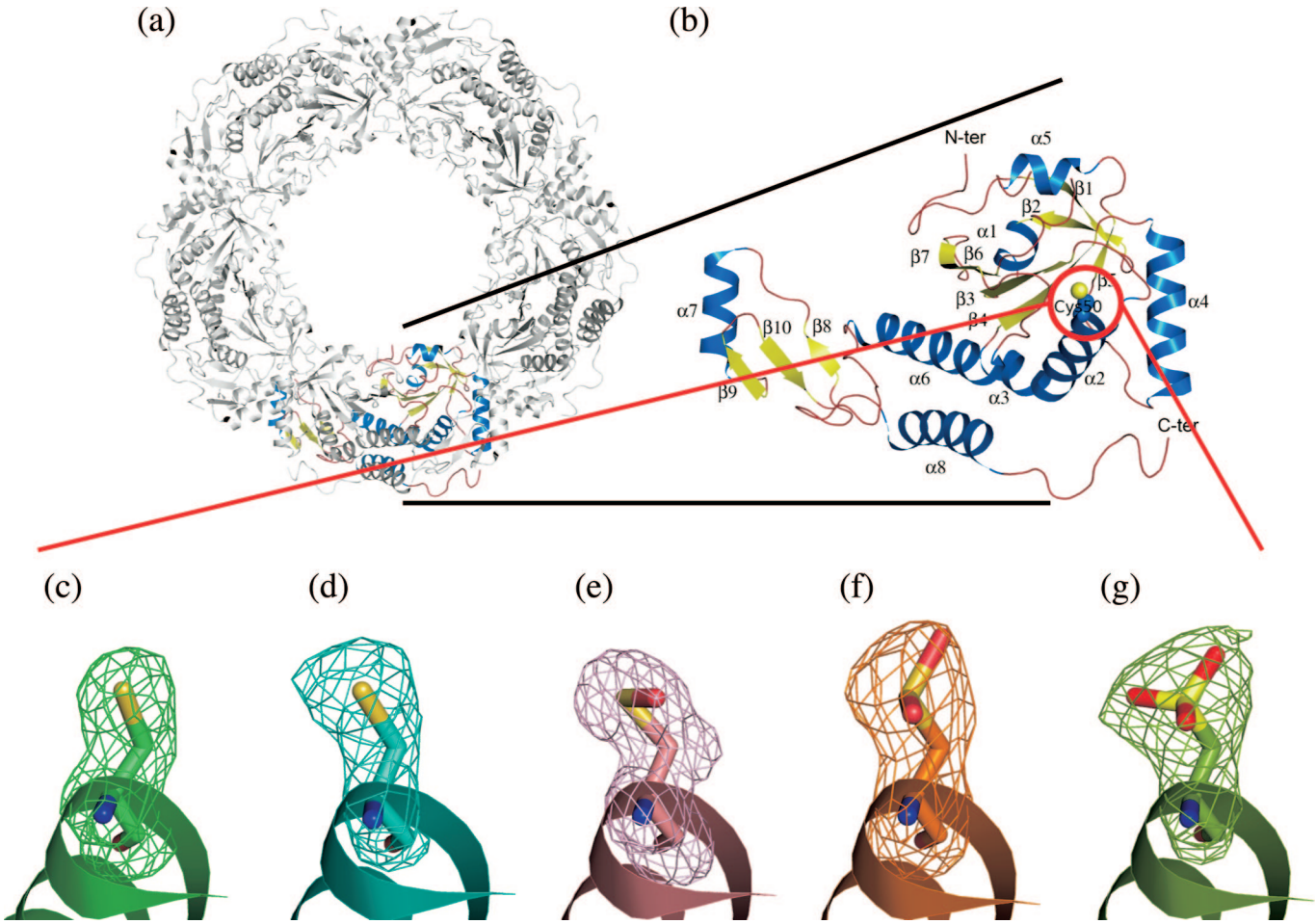

Fig. S1. Changes in the peroxidatic cysteine of ApTPx during H_2O_2-mediated oxidation. The decameric and monomeric structures of ApTPx in the reduced form are shown in *a* and *b*, respectively. In *b*, the peroxidatic cysteine residue is indicated by a red circle. Shown are the side chains of the peroxidatic cysteine in the reduced (*c*), preoxidation (*d*), hypervalent sulfur (*e*), sulfinic acid (*f*), and sulfonic acid (*g*) forms of ApTPx. In *e*, the side chain of His-42 is excluded from the drawing although it is covalently connected with the S^{γ} atom of C_p50. The C_p residues are imposed onto $|F_o| - |F_c|$ omit maps of the corresponding residues contoured at 3σ. All structures are drawn from the same direction.

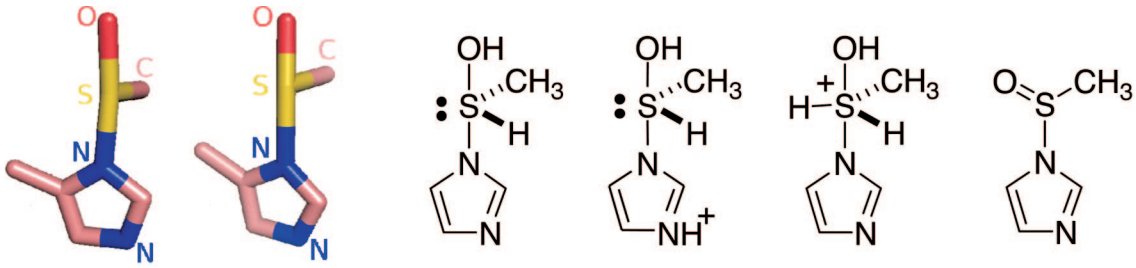

	Form 1	Form 2	Model 1	Model 2	Model 3	Model 4
angle (O-S-C, °)	90.0 ± 4.4	81.3 ± 2.8	91.5	93.7	87.8	106.55
angle (O-S-N, °)	173.3 ± 4.4	170.2 ± 4.5	170.3	172.4	174.1	109.9
angle (N-S-C, °)	90.8 ± 4.4	99.9 ± 3.7	88.2	89	98	95.29
distance (O-S, Å)	1.85 ± 0.08	1.72 ± 0.01	1.8	1.68	1.7	1.49
distance (S-N, Å)	2.15 ± 0.13	2.21 ± 0.13	1.97	2.39	1.77	1.77

Fig. S2. Comparisons of observed and calculated structures. Values for the crystal structure (forms 1 and 2) are the average ± SD of the 10 subunits. The columns of models 1–4 show the calculated values of each model.

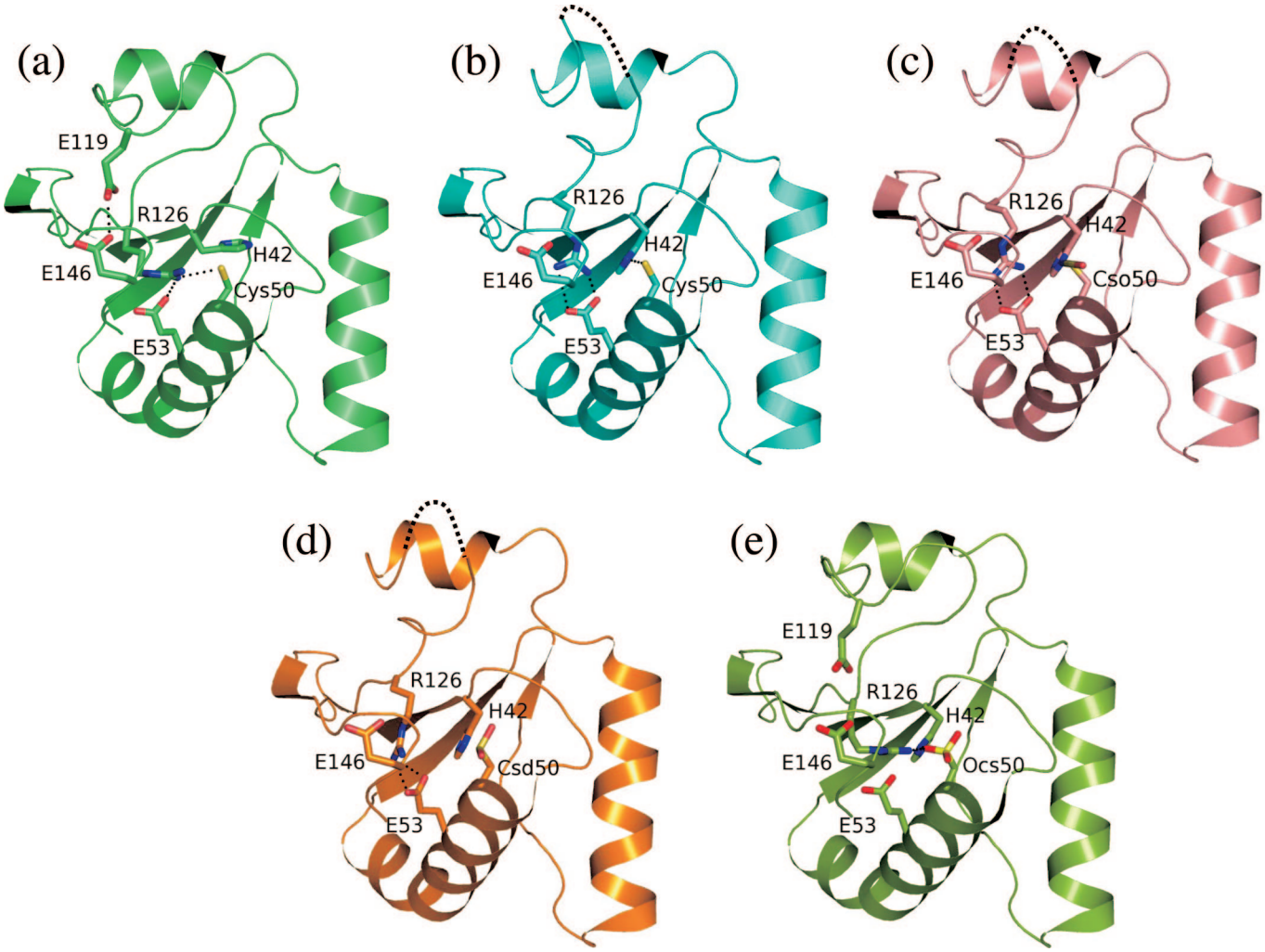

Fig. S3. Conformational variations of ApTPx. Shown are the chain conformations around the peroxidatic cysteine of ApTPx in reduced (*a*), preoxidation (*b*), hypervalent sulfur (*c*), sulfinic acid (*d*), and sulfonic acid (*e*) forms. Dashed lines in *b*–*d* show the disordered loop. All structures are drawn from the same direction as Fig. S1.

Table S1. Data collection and refinement statistics

	Preoxidation	Hypervalent sulfur	Sulfinic acid	Sulfenic acid
Data collection				
Unit cell, Å	$a = 76.20$, $b = 103.35$, $c = 104.63$, $\alpha = 105.79$, $\beta = 105.19$, $\gamma = 92.68$	$a = 76.01$, $b = 102.97$, $c = 104.35$, $\alpha = 105.83$, $\beta = 105.30$, $\gamma = 92.69$	$a = 76.23$, $b = 102.97$, $c = 104.77$, $\alpha = 105.81$, $\beta = 105.20$, $\gamma = 92.58$	$a = 76.20$ $b = 103.35$, $c = 104.63$, $\alpha = 105.79$, $\beta = 105.19$, $\gamma = 92.68$
Z	10	10	10	10
Space group	$P1$	$P1$	$P1$	$P1$
V_M	2.66	2.63	2.65	2.65
Resolution range, Å	19.99–2.4 (2.49–2.40)	50.00–1.77 (1.83–1.77)	40.00–2.85 (2.95–2.85)	98.53–2.35 (2.43–2.35)
R_{merge}, %*†	8.8 (22.6)	5.8 (38.4)	10.9 (38.6)	6.7 (30.5)
Completeness, %	87.2 (71.4)	95.0 (81.7)	97.7 (89.7)	97.0 (87.8)
Unique reflections	100,947 (8,275)	269,621 (23,152)	66,741 (6,134)	116,808 (10,556)
Redundancy	2.4 (1.9)	1.9 (1.6)	2.1 (2.0)	2.1 (1.9)
$I/\sigma(I)$	9.0 (2.9)	10.0 (1.4)	6.4 (2.0)	8.7 (2.4)
Refinement				
Resolution range, Å	19.99–2.4	49.15–1.77	39.37–2.85	98.53–2.35
No. of reflections	95,723	255,882	63,393	110,905
R_{cryst}(%) / R_{free} (%)‡§	15.67 / 22.95	18.8 / 22.0	19.8 / 24.5	16.6 / 21.9
rmsd bond length, Å	0.024	0.015	0.023	0.024
rmsd bond angle, °	2.14	1.48	1.90	2.00
Protein atoms	19,355	19,220	19,347	19,635
Water molecules	542	1,821	0	705
Ramachandran plot, %¶				
Favored	89.2	91.6	87.2	88.7
Allowed	9.5	7.9	12.5	9.8

*Values in parentheses are for the highest-resolution shell.
†$R_{merge} = = \Sigma |I - \langle I \rangle| / \Sigma I$, where I is the intensity of observation I and $\langle I \rangle$ is the mean intensity of the reflection.
‡$R_{cryst} = \Sigma \| F_o| - |F_c| \| / \Sigma |F_o|$, where F_o and F_c are the observed and calculated structure factor amplitudes, respectively.
§R_{free} was calculated by using a randomly selected 5% of the dataset that was omitted through all stages of refinement.
¶Ramachandran plot was performed for all residues other than Gly and Pro.